

Hydroxyapatite-Supported Palladium Nanoclusters: A Highly Active Heterogeneous Catalyst for Selective Oxidation of Alcohols by Use of Molecular Oxygen

Kohsuke Mori, Takayoshi Hara, Tomoo Mizugaki, Kohki Ebitani, and Kiyotomi Kaneda*

Contribution from the Department of Materials Engineering Science, Graduate School of Engineering Science, Osaka University, 1-3 Machikaneyama, Toyonaka, Osaka 560-8531, Japan

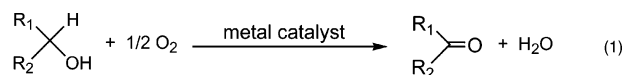
Received February 28, 2004; E-mail: kaneda@cheng.es.osaka-u.ac.jp

Abstract: Treatment of a stoichiometric hydroxyapatite (HAP), $\text{Ca}_{10}(\text{PO}_4)_6(\text{OH})_2$, with $\text{PdCl}_2(\text{PhCN})_2$ gives a new type of palladium-grafted hydroxyapatite. Analysis by means of powder X-ray diffraction (XRD), X-ray photoelectron spectroscopy (XPS), energy-dispersive X-ray (EDX), IR, and Pd K-edge X-ray absorption fine structure (XAFS) proves that a monomeric PdCl_2 species is chemisorbed on the HAP surface, which is readily transformed into Pd nanoclusters with a narrow size distribution in the presence of alcohol. Nanoclustered Pd^0 species can effectively promote the alcohol oxidation under an atmospheric O_2 pressure, giving a remarkably high turnover number (TON) of up to 236 000 with an excellent turnover frequency (TOF) of approximately 9800 h^{-1} for a 250- μmol -scale oxidation of 1-phenylethanol under solvent-free conditions. In addition to advantages such as a simple workup procedure and the ability to recycle the catalyst, the present Pd catalyst does not require additives to complete the catalytic cycle. The diameters of the generated Pd nanoclusters can be controlled upon acting on the alcohol substrates used. Oxidation of alcohols is proposed to occur primarily on low-coordination sites within a regular arrangement of the Pd nanocluster by performing calculations on the palladium crystallites.

Introduction

The selective oxidation of alcohols is widely recognized as one of the most fundamental transformations in both laboratory and industrial synthetic chemistry because the corresponding carbonyl compounds serve as important and versatile intermediates for the synthesis of fine chemicals.¹ Many oxidizing reagents including permanganate and dichromate have been traditionally employed in order to accomplish this transformation.² These stoichiometric oxidants, however, feature the serious drawbacks that they are expensive and/or toxic and produce a large amount of wastes. With ever-increasing environmental concerns, much attention has been directed toward the development of promising catalytic protocols that use molecular oxygen as a primary oxidant, which is readily available and produces water as the sole byproduct.³ Accordingly, a remarkable number

of metal-catalyzed aerobic processes, especially based on Pd ,⁴ Ru ,⁵ and Cu ⁶ complexes, have been developed in recent years (eq 1).



$\text{R}_1, \text{R}_2 = \text{H, alkyl, aryl}$

Since the first successful example of palladium-catalyzed aerobic oxidation of alcohols in 1977 by Blackburn and Schwartz,^{4a} subsequent efforts have extended the substrate scope and efficiency of palladium catalysts. Of the reported systems, the combination of simple Pd^{II} salts and pyridine or bidentate nitrogen ligands has been extensively explored for this transformation including oxidative kinetic resolution of *secondary*

- (1) (a) Sheldon, R. A.; Kochi, J. K. *Metal-Catalyzed Oxidations of Organic Compounds*; Academic Press: New York, 1981. (b) Hill, C. L. *Advances in Oxygenated Processes*, Baumstark, A. L., Ed.; JAI Press: London, 1988; Vol. 1, p 1. (c) Hudlucky, M. *Oxidations in Organic Chemistry*; ACS Monograph Series; American Chemical Society: Washington, DC, 1990. (d) *Comprehensive Organic Synthesis*; Trost, B. M., Fleming, I., Eds.; Pergamon: Oxford, U.K., 1991. (e) Parshall, G. W.; Ittel, S. D. *Heterogeneous Catalysis*, 2nd ed.; John Wiley & Sons: New York, 1992.
- (2) (a) Cainelli, G.; Cardillo, G. *Chromium Oxidants in Organic Chemistry*; Springer: Berlin, 1984. (b) Lee, D. G.; Spitzer, U. A. *J. Org. Chem.* **1970**, *35*, 3589. (c) Menger, F. M.; Lee, C. *Tetrahedron Lett.* **1981**, *22*, 1655.
- (3) (a) Trost, B. M. *Science* **1991**, *254*, 1471. (b) Anastas, P. T.; Warner, J. C. *Green Chemistry, Theory and Practice*; Oxford University Press: Oxford, U.K., 1998. (c) Clark, J. H. *Green Chem.* **1999**, *1*, 1. (d) Sheldon, R. A. *Green Chem.* **2000**, *2*, G1. (e) Anastas, P. T.; Bartlett, L. B.; Kirchhoff, M. M.; Williamson, T. C. *Catal. Today* **2000**, *55*, 11.

- (4) (a) Blackburn, T. F.; Schwartz, J. *J. Chem. Soc., Chem. Commun.* **1977**, 157. (b) Gómez-Bengoia, E.; Noheda, P.; Echavarren, A. M. *Tetrahedron Lett.* **1994**, *35*, 7097. (c) Aiet-Mohand, S.; Henin, F.; Muzart, J. *Tetrahedron Lett.* **1995**, *36*, 2473. (d) Kaneda, K.; Fujii, M.; Morioka, K. *J. Org. Chem.* **1996**, *61*, 4502. (e) Kaneda, K.; Fujie, Y.; Ebitani, K. *Tetrahedron Lett.* **1997**, *38*, 9023. (f) Peterson, K. P.; Larock, R. C. *J. Org. Chem.* **1998**, *63*, 3185. (g) Nishimura, T.; Onoue, T.; Ohe, K.; Uemura, S. *Tetrahedron Lett.* **1998**, *39*, 6011. (h) Nishimura, T.; Onoue, T.; Ohe, K.; Uemura, S. *J. Org. Chem.* **1999**, *64*, 6750. (i) ten Brink, G.-J.; Arends, I. W. C. E.; Sheldon, R. A. *Science* **2000**, *287*, 1636. (j) Stahl, S. S.; Thorman, J. L.; Nelson, R. C.; Kozee, M. A. *J. Am. Chem. Soc.* **2001**, *123*, 7188. (k) Steinhoff, M. A.; Fix, S. R.; Stahl, S. S. *J. Am. Chem. Soc.* **2002**, *124*, 766. (l) ten Brink, G.-J.; Arends, I. W. C. E.; Sheldon, R. A. *Adv. Synth. Catal.* **2002**, *344*, 355. (m) Steinhoff, B. A.; Stahl, S. S. *Org. Lett.* **2002**, *4*, 4179. (n) Schultz, M. J.; Park, C. C.; Sigman, M. S. *Chem. Commun.* **2002**, 3034. (o) Jensen, D. R.; Schultz, M. J.; Mueller, J. A.; Sigman, M. S. *Angew. Chem., Int. Ed.* **2003**, *42*, 3810.

alcohols.⁷ However, they often require high catalyst concentrations, an excess of ligands or bases, and high oxygen pressures. In addition, the use of homogeneous metal catalysts on an industrial scale is limited by practical problems due to the difficulties in recovering the expensive catalyst metals and ligands from the reaction mixture. In this context, the current research has been focused on the development of efficient heterogeneous catalysts possessing superior activity as well as high reusability.⁸ Although some progress has been achieved by heterogeneous Ru catalysts,⁹ only a few heterogeneous Pd ones are available to date, for example, Pd on activated carbon,¹⁰ Pd on pumice,¹¹ Pd-hydroxalcalite,¹² Pd on TiO₂,¹³ and polymer-supported Pd.¹⁴ Unfortunately, these heterogeneous Pd systems suffer from low catalytic activities and a limited substrate scope.

Hydroxyapatites possess Ca²⁺ sites surrounded by PO₄³⁻ tetrahedra parallel to the hexagonal axis, which have attracted considerable interest in view of their potential usefulness as

biomaterials, adsorbents, and ion exchangers. However, few excellent applications as catalysts or catalyst supports have emerged so far.¹⁵ We have recently disclosed a new strategy for the design of high-performance heterogeneous catalysts utilizing the hydroxyapatite as a macroligand for catalytically active centers.¹⁶ The introduction of transition metal cations, such as Ru and Pd, into the apatite framework could generate stable monomeric phosphate complexes, which exhibited prominent catalytic performances for various oxidation reactions using molecular oxygen^{16a-d} and for carbon-carbon bond-forming reactions.^{16d,g} Herein, we present the synthesis and characterization of the palladium-grafted hydroxyapatite and its evaluation as a heterogeneous catalyst for the oxidation of alcohols by use of molecular oxygen. The in situ generated Pd nanocluster on the hydroxyapatite surface has proven to be effective as a catalytically active species for selective and environmentally benign alcohol oxidation. We also mention the interesting aspects such as substrate scope and recycling of the catalyst as well as size effect of the formed Pd nanoclusters on the catalytic activities.

Results and Discussion

Catalyst Preparation and Characterization. The choice of hydroxyapatites as catalyst supports is motivated by the following advantages:¹⁶ (i) well-defined monomeric active species can be immobilized on their surface, on the basis of high ion-exchange ability and adsorption capacity; (ii) nonporous structure can help to overcome the problems toward mass transfer limitation; and (iii) weak acid-base properties prohibit side reactions induced by the support itself. To obtain a highly active heterogeneous Pd catalyst for aerobic alcohol oxidation, we synthesized two types of hydroxyapatite-supported Pd catalysts designed with strict compositional control of the hydroxyapatites.

Hydroxyapatites [HAP; Ca_{10-*Z*}(HPO₄)_{*Z*}(PO₄)_{6-*Z*}(OH)_{2-*Z*} (0 ≤ *Z* ≤ 1; 1.5 ≤ Ca/P ≤ 1.67)] were synthesized from Ca-(NO₃)₂·4H₂O and (NH₄)₂HPO₄ by the precipitation method according to a literature procedure.¹⁷ Selecting an appropriate Ca/P molar ratios in the preparation sequence yielded the stoichiometric hydroxyapatite Ca₁₀(PO₄)₆(OH)₂ (HAP-0; *Z* = 0, Ca/P = 1.67) and the nonstoichiometric Ca-deficient hydroxyapatite Ca₉(HPO₄)(PO₄)₅(OH) (HAP-1; *Z* = 1, Ca/P = 1.50), respectively. The crystallographic structure of the Ca-deficient hydroxyapatite is identical to that of the stoichiometric one, and its charge deficiency due to the lack of Ca²⁺ in the lattice is compensated by introduction of H⁺ into the PO₄³⁻ ion and removal of OH⁻ in the parent unit cell.¹⁵ The prepared HAPs (HAP-0 and HAP-1) were characterized by powder X-ray diffraction (XRD), infrared spectroscopy (IR), and elemental analysis.

- (5) (a) Tang, R.; Diamond, S. E.; Neary, N.; Mares, F. *J. Chem. Soc., Chem. Commun.* **1978**, 562. (b) Bilgrien, C.; Davis, S.; Drago, R. S. *J. Am. Chem. Soc.* **1987**, *109*, 3786. (c) Bäckvall, J.-E.; Chowdhury, R. L.; Karlsson, U. *J. Chem. Soc., Chem. Commun.* **1991**, 473. (d) Iwahama, T.; Sakaguchi, S.; Nishiyama, Y.; Ishii, Y. *Tetrahedron Lett.* **1995**, *36*, 6923. (e) Lenz, R.; Ley, S. V. *J. Chem. Soc., Perkin Trans. 1* **1997**, 3291. (f) Markó, I. E.; Giles, P. R.; Tsukazaki, M.; Chellé-Regnaut, I.; Urch, C. J.; Brown, S. M. *J. Am. Chem. Soc.* **1997**, *119*, 12661. (g) Hanyu, A.; Takezawa, E.; Sakaguchi, S.; Ishii, Y. *Tetrahedron Lett.* **1998**, *39*, 5557. (h) Coleman, K. S.; Lorber, C. Y.; Osborn, J. A. *Eur. J. Inorg. Chem.* **1998**, 1673. (i) Lee, M.; Chang, S. *Tetrahedron Lett.* **2000**, *41*, 7507. (j) Shapley, P. A.; Zhang, N.; Allen, J. L.; Pool, D. H.; Liang, H.-C. *J. Am. Chem. Soc.* **2000**, *122*, 1079. (k) Dijkman, A.; Marino-Gonzalez, A.; Payeras, A. M. I.; Arends, I. W. C. E.; Sheldon, R. A. *J. Am. Chem. Soc.* **2001**, *123*, 6826. (l) Csornyik, G.; Ell, A. H.; Fadini, L.; Pugin, B.; Bäckvall, J.-E. *J. Org. Chem.* **2002**, *67*, 1657.
- (6) (a) Markó, I. E.; Giles, P. R.; Tsukazaki, M.; Brown, S. M.; Urch, C. J. *Science* **1996**, *274*, 2044. (b) Markó, I. E.; Tsukazaki, M.; Giles, P. R.; Brown, S. M.; Urch, C. J. *Angew. Chem. Int. Ed.* **1997**, *36*, 2208. (c) Wang, Y.; Dubois, J. L.; Hedman, B.; Hodgson, K. O.; Stack, T. D. P. *Science* **1998**, *279*, 537. (d) Markó, I. E.; Gautier, A.; Chellé-Regnaut, I.; Giles, P. R.; Tsukazaki, M.; Urch, C. J.; Brown, S. M. *J. Org. Chem.* **1998**, *63*, 7576. (e) Markó, I. E.; Giles, P. R.; Tsukazaki, M.; Gautier, A.; Chellé-Regnaut, I.; Brown, S. M.; Urch, C. J. *J. Org. Chem.* **1999**, *64*, 2433. (f) Gamez, P.; Arends, I. W. C. E.; Reedijk, J.; Sheldon, R. A. *Chem. Commun.* **2003**, 2414.
- (7) Pd-catalyzed alcohol oxidation for kinetic resolution, see (a) Jensen, D. R.; Pugsley, J. S.; Sigman, M. S. *J. Am. Chem. Soc.* **2001**, *123*, 7475. (b) Ferreira, E. M.; Stoltz, B. M. *J. Am. Chem. Soc.* **2001**, *123*, 7725. (c) Mueller, J. A.; Jensen, D. R.; Sigman, M. S. *J. Am. Chem. Soc.* **2002**, *124*, 8202. (d) Jensen, D. R.; Sigman, M. S. *Org. Lett.* **2003**, *5*, 63. (e) Bagdanoff, J. T.; Ferreira, E. M.; Stoltz, B. M. *Org. Lett.* **2003**, *5*, 835. (f) Mandal, S. K.; Jensen, D. R.; Pugsley, J. S.; Sigman, M. S. *J. Org. Chem.* **2003**, *68*, 4600. (g) Mueller, J. A.; Sigman, M. S. *J. Am. Chem. Soc.* **2003**, *125*, 7005. (h) Mandal, S. K.; Sigman, M. S. *J. Org. Chem.* **2003**, *68*, 7535.
- (8) Sheldon, R. A.; Wallau, M.; Arends, I. W. C. A.; Schuchardt, U. *Acc. Chem. Res.* **1998**, *31*, 485.
- (9) (a) Hinzen, B.; Ley, S. V. *J. Chem. Soc., Perkin Trans. 1* **1997**, 1707. (b) Vocanson, F.; Guo, Y. P.; Namy, J. L.; Kagan, H. B. *Synth. Commun.* **1998**, *28*, 2577. (c) Kaneda, K.; Yamashita, T.; Matsushita, T.; Ebitani, K. *J. Org. Chem.* **1998**, *67*, 1750. (d) Matsushita, T.; Ebitani, K.; Kaneda, K. *Chem. Commun.* **1999**, 265. (e) Bleloch, A.; Johnson, B. F. G.; Ley, S. V.; Price, A. J.; Shephard, D. S.; Thomas, A. W. *Chem. Commun.* **1999**, 1907. (f) Choi, E.; Lee, C.; Na, Y.; Chang, S. *Org. Lett.* **2002**, *4*, 2369. (g) Ji, H.-B.; Mizugaki, T.; Ebitani, K.; Kaneda, K. *Tetrahedron Lett.* **2002**, *43*, 7179. (h) Ji, H.-B.; Ebitani, K.; Mizugaki, T.; Kaneda, K. *Catal. Commun.* **2002**, *3*, 511. (i) Yamaguchi, K.; Mizuno, N. *Angew. Chem., Int. Ed.* **2002**, *41*, 4538. (j) Zhan, B.-Z.; White, M. A.; Sham, T.-K.; Pincock, J. A.; Doucet, R. J.; Rao, K. V. R.; Robertson, K. N.; Cameron, T. S. *J. Am. Chem. Soc.* **2003**, *125*, 2195. (k) Yamaguchi, K.; Mizuno, N. *Chem. Eur. J.* **2003**, *9*, 4353. (l) Ciriminna, R.; Pagliaro, M. *Chem. Eur. J.* **2003**, *9*, 5067. (m) Ebitani, K.; Ji, H.-B.; Mizugaki, T.; Kaneda, K. *J. Mol. Catal. A: Chem.* **2004**, *212*, 161.
- (10) Mallat, T.; Baiker, A. *Catal. Today* **1994**, *19*, 247.
- (11) Liotta, L. F.; Venezia, A. M.; Deganello, G.; Longo, A.; Martorana, A.; Schay, Z.; Guzzi, L. *Catal. Today* **2001**, *66*, 271.
- (12) (a) Nishimura, T.; Kakiuchi, N.; Inoue, M.; Uemura, S. *Chem. Commun.* **2000**, 1245. (b) Kakiuchi, N.; Maeda, Y.; Nishimura, T.; Uemura, S. *J. Org. Chem.* **2001**, *66*, 6220.
- (13) (a) Ebitani, K.; Fujie, Y.; Kaneda, K. *Langmuir* **1999**, 1907. (b) Choi, K.-M.; Akita, T.; Mizugaki, T.; Ebitani, K.; Kaneda, K. *New J. Chem.* **2003**, *27*, 324.
- (14) (a) Uozumi, Y.; Nakao, R. *Angew. Chem., Int. Ed.* **2003**, *42*, 194. (b) Corain, B.; Jerabek, K.; Centomo, P.; Canton, P. *Angew. Chem., Int. Ed.* **2004**, *43*, 959.
- (15) Elliott, J. C. *Structure and Chemistry of the Apatites and Other Calcium Orthophosphates*; Elsevier: Amsterdam, 1994.
- (16) (a) Yamaguchi, K.; Mori, K.; Mizugaki, T.; Ebitani, K.; Kaneda, K. *J. Am. Chem. Soc.* **2000**, *122*, 7144. (b) Mori, K.; Yamaguchi, K.; Mizugaki, T.; Ebitani, K.; Kaneda, K. *Chem. Commun.* **2001**, 461. (c) Mori, K.; Tano, M.; Mizugaki, T.; Ebitani, K.; Kaneda, K. *New J. Chem.* **2002**, *26*, 1536. (d) Mori, K.; Yamaguchi, K.; Hara, T.; Mizugaki, T.; Ebitani, K.; Kaneda, K. *J. Am. Chem. Soc.* **2002**, *124*, 11572. (e) Murata, M.; Hara, T.; Mori, K.; Ooe, M.; Mizugaki, T.; Ebitani, K.; Kaneda, K. *Tetrahedron Lett.* **2003**, *44*, 4981. (f) Hara, T.; Mori, K.; Ooe, M.; Mizugaki, T.; Ebitani, K.; Kaneda, K. *Tetrahedron Lett.* **2003**, *44*, 6207. (g) Mori, K.; Hara, T.; Mizugaki, T.; Ebitani, K.; Kaneda, K. *J. Am. Chem. Soc.* **2003**, *125*, 11460.
- (17) Sugiyama, S.; Minami, T.; Hayashi, H.; Tanaka, M.; Shigemoto, N.; Moffat, J. B. *J. Chem. Soc., Faraday Trans.* **1996**, *92*, 293.

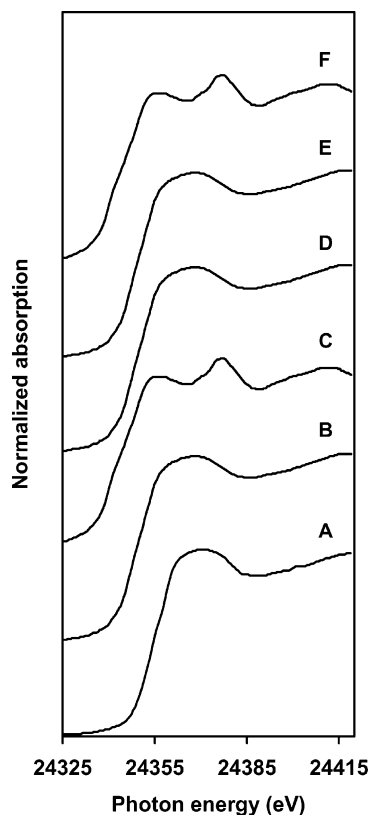


Figure 1. Pd K-edge XANES spectra of (A) PdHAP-0, (B) PdHAP-1, (C) recovered PdHAP-0, (D) recovered PdHAP-1 for the oxidation of 1-phenylethanol, (E) Pd oxide, and (F) Pd foil. Reactions were conducted with 1-phenylethanol (1 mmol), PdHAP (0.1 g, Pd 2 μ mol), and trifluorotoluene (5 mL) at 90 °C for 1 h under an O₂ atmosphere.

Immobilization of the palladium precursor on the HAPs was achieved by the impregnation method in organic solvents. Treatment of the HAP-0 with an acetone solution of PdCl₂(PhCN)₂ for 3 h at room temperature yielded PdHAP-0 (Pd content 0.02 mmol·g⁻¹) as a pale yellow powder, while PdHAP-1 (Pd content 0.02 mmol·g⁻¹) was obtained as a white powder by the same method with HAP-1. The Brunauer–Emmett–Teller (BET) surface areas of these samples were found to be 48.8 and 48.4 m²·g⁻¹, respectively.

To gain insight into the structures of surface-bound Pd species of the PdHAPs (PdHAP-0 and PdHAP-1), characterization by physicochemical methods was performed. XRD revealed that the PdHAPs and the parent HAPs had the same structures. The presence of chlorine in PdHAP-0 was confirmed by X-ray photoelectron spectroscopy (XPS) and energy-dispersive X-ray (EDX) spectroscopy; the atomic ratio of Pd to Cl was determined to be 1:2, while chlorine was not detected in PdHAP-1. No signals assignable to the $\nu(\text{CN})$ band could be observed in IR spectroscopy, suggesting that PhCN ligands originating from the Pd precursor were not involved in the immobilized Pd species. The absence of carbon and nitrogen atoms in the PdHAPs was also evidenced by CHN elemental analysis. Inductively coupled plasma (ICP) analysis revealed that no Ca was present in the filtrate after the palladium loading. Therefore, isomorphic substitution of Pd for Ca did not occur in the above preparation sequence utilizing organic solvents, which is in sharp contrast to our result for previously prepared Ru-exchanged hydroxyapatite via the cation-exchange method in an aqueous medium.^{16a} Figure 1 shows the Pd K-edge X-ray absorption

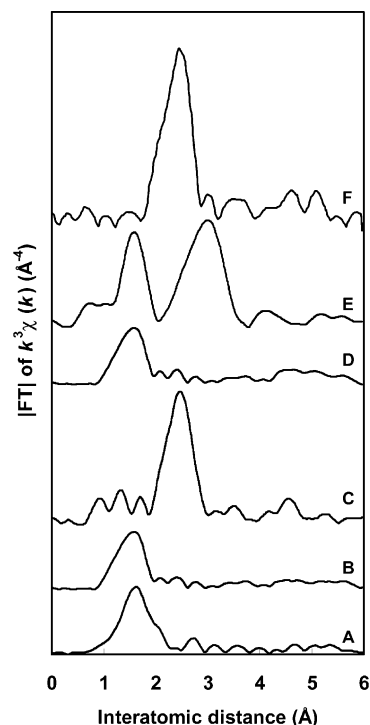


Figure 2. Fourier transforms of k^3 -weighted Pd K-edge EXAFS experimental data for (A) PdHAP-0, (B) PdHAP-1, (C) recovered PdHAP-0, (D) recovered PdHAP-1 for the oxidation of 1-phenylethanol, (E) Pd oxide, and (F) Pd foil. Phase shift was not corrected. Reactions were conducted with 1-phenylethanol (1 mmol), PdHAP (0.1 g, Pd 2 μ mol), and trifluorotoluene (5 mL) at 90 °C for 1 h under an O₂ atmosphere.

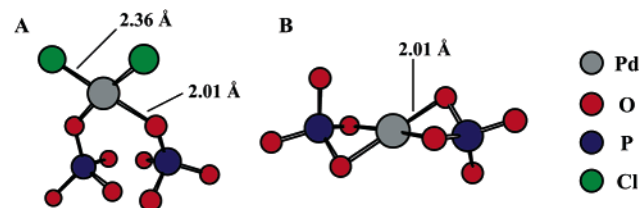
near-edge structure (XANES) spectra of the PdHAPs, together with Pd oxide and Pd foil as reference samples. The shapes of the XANES spectra and the edge position in both PdHAPs (A and B) were identical to those of Pd oxide (E) but differed from those of Pd foil (F), which reveals that all Pd species are in the 2+ oxidation state. The Fourier transforms (FT) of k^3 -weighted extended X-ray absorption fine structure (EXAFS) data are depicted in Figure 2. No peaks due to Pd–Pd and Pd–O–Pd bonds in the second coordination sphere, detectable in those of Pd foil and Pd oxide at around 2.5 and 3.0 Å, were observed for both PdHAPs (A and B versus E and F). The inverse Fourier transform (FT) of the peaks around 1–2 Å for PdHAP-0 was well fitted with two chloride atoms at a Pd–Cl distance of 2.36 Å and two oxygen atoms at a Pd–O distance of 2.01 Å (Table 1, sample A).¹⁸ On the other hand, the best fit for PdHAP-1 was achieved with only a Pd–O bond having an interatomic distance (R) and a coordination number (CN) of 2.01 Å and 4, respectively (Table 1, sample B).¹⁸ The distances from Pd to Cl and to the nearest O atoms were essentially consistent with the values for the Pd–Cl bond ($R = 2.33$ Å) in PdCl₂ and the Pd–O bond ($R = 2.02$ Å) in Pd oxide. The second neighboring Pd–O bonds were assigned to the weak interaction between Pd and PO₄³⁻ ions of hydroxyapatites. On the basis of these results, we can propose the most reasonable surface structure for the PdHAPs, as illustrated in Figure 3. A monomeric PdCl₂ species is grafted by chemisorption on the P=O groups of the HAP-0 surface (A), whereas a coordinately saturated monomeric Pd^{II} phosphate complex surrounded by four oxygen atoms is formed at the Ca-deficient site of HAP-1 (B). The present simple

(18) See Supporting Information.

Table 1. Curve-Fitting Analysis for PdHAP Catalysts^a

| sample | shell | CN ^b | <i>R</i> ^c (Å) | $\Delta\sigma^d$ (Å ²) |
|-----------------------|---------|-----------------|---------------------------|------------------------------------|
| PdHAP-0 (A) | Pd–Cl | 2.0 | 2.36 | 0.0087 |
| | Pd–O(1) | 2.1 | 2.01 | 0.0006 |
| | Pd–O(2) | 3.0 | 2.37 | 0.0199 |
| PdHAP-1 (B) | Pd–O(1) | 4.2 | 2.01 | 0.0031 |
| | Pd–O(2) | 3.0 | 2.34 | 0.0342 |
| recovered PdHAP-0 (C) | Pd–Pd | 10.0 | 2.76 | 0.0018 |
| recovered PdHAP-1 (D) | Pd–O(1) | 4.1 | 2.01 | 0.0020 |
| | Pd–O(2) | 3.0 | 2.33 | 0.0233 |

^a Inverse Fourier transformations were performed for the regions of 0.9–2.2 Å in Figure 1A, 0.9–2.0 Å in Figure 1B, 1.95–3.0 Å in Figure 1C, and 0.9–2.0 Å in Figure 1D. ^b Coordination number. ^c Interatomic distance. ^d Difference between Debye–Waller factor of PdHAP and that of the reference sample.

**Figure 3.** Proposed surface structures around Pd^{II} center of PdHAP-0 (A) and PdHAP-1 (B). The nearest oxygen and chlorine atoms around the Pd^{II} are shown.

preparation method based on precise control of the Ca/P ratios of the parent hydroxyapatites enables a strong protocol to create two unique monomeric Pd species with intrinsically different surroundings on solid surfaces.

The calculated PO₄³⁻ ion coverage on the surface of hydroxyapatites is 5 PO₄³⁻/nm²,¹⁹ which is roughly estimated to be 0.42 mmol·g⁻¹ for this surface area. However, the maximum Pd loadings were limited to only 0.02 mmol·g⁻¹ for both PdHAPs; excess Pd complex could be recovered from the acetone solution. This finding indicates that the Pd species may be located on specific sites of the hydroxyapatite surface with appropriate distances and arrangements between the two adjacent PO₄³⁻ ions.

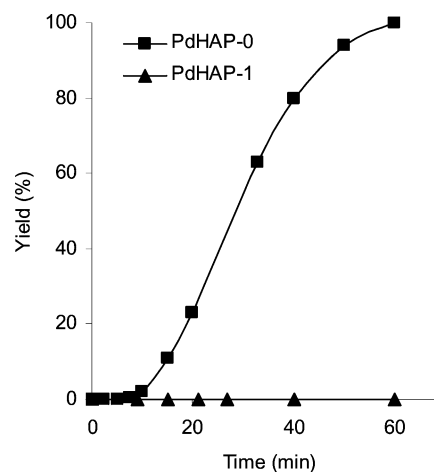
Active Pd Species for Aerobic Oxidation of Alcohols. In an effort to compare the potential abilities of these PdHAPs with those of other commercially available Pd catalysts, oxidations of various alcohols were carried out under atmospheric O₂ pressure. The results are summarized in Table 2. The PdHAP-0 catalyst exhibited the highest activity with respect to both conversion and selectivity. Oxidation of benzyl alcohol by use of Pd/Al₂O₃ and Pd/SiO₂ showed relatively high conversions; however, benzyl benzoate was obtained as a side product (entries 4 and 5). In the case of cinnamyl alcohol, the presence of an allylic C=C double bond did not affect the catalytic efficiency of PdHAP-0 (entry 11), whereas Pd/carbon and Pd/Al₂O₃ were less selective, affording a mixture of 3-phenyl-1-propanal, 3-phenyl-1-propanol, and cinnamaldehyde (entries 13 and 14). It is important to note that oxidation of alcohols hardly occurred in the presence of PdHAP-1.

The time course for the oxidation of 1-phenylethanol was monitored periodically, as shown in Figure 4. PdHAP-0 had an induction period of about 10 min, in which a concomitant color change of the catalyst from yellow to light gray was observed and then no noticeable O₂ absorption was detected. After the

Table 2. Oxidation of Benzyl Alcohol, 1-Phenylethanol, and Cinnamyl Alcohol by Various Palladium Catalysts with Molecular Oxygen^a

| entry | substrate | catalyst | conv. (%) ^b | yield (%) ^b |
|-----------------|-----------|--|------------------------|------------------------|
| 1 | | PdHAP-0 | >99 | 99 |
| 2 | | PdHAP-1 | no reaction | •• |
| 3 | | Pd/carbon ^c | 46 | 42 |
| 4 | | Pd/Al ₂ O ₃ ^c | 96 | 38 ^d |
| 5 | | Pd/SiO ₂ ^c | 71 | 47 ^d |
| 6 | | PdHAP-0 | >99 | 99 |
| 7 | | PdHAP-1 | no reaction | •• |
| 8 | | Pd/carbon ^c | 11 | 10 |
| 9 | | Pd/Al ₂ O ₃ ^c | 76 | 76 |
| 10 | | Pd/SiO ₂ ^c | 4 | 4 |
| 11 ^e | | PdHAP-0 | 91 | 87 |
| 12 ^e | | PdHAP-1 | no reaction | •• |
| 13 ^e | | Pd/carbon ^c | 90 | 68 ^f |
| 14 ^e | | Pd/Al ₂ O ₃ ^c | 83 | 66 ^f |
| 15 ^e | | Pd/SiO ₂ ^c | 31 | 30 |

^a Reaction conditions: alcohol (1 mmol), palladium catalyst (0.2 mol %), trifluorotoluene (5 mL), 90 °C, 1 h, O₂ atmosphere. ^b Determined by GC via an internal standard technique. ^c 0.5 wt % Pd. Purchased from N. E. Chemcat. ^d Benzyl benzoate was formed. ^e Toluene was used as solvent; 6 h. ^f 3-Phenyl-1-propanal and 3-phenyl-1-propanol were formed.

**Figure 4.** Time profile for the oxidation of 1-phenylethanol catalyzed by PdHAP. Reaction conditions: PdHAP (0.1 g, Pd 2 μmol), 1-phenylethanol (1 mmol), trifluorotoluene (5 mL), 90 °C, O₂ atmosphere.

induction period, consumption of molecular oxygen began, and finally the molar ratio of O₂ uptake to acetophenone yield was ca. 1:2. On the other hand, neither color change nor O₂ uptake occurred in the case of PdHAP-1. The whole of these data suggest that the reaction medium transforms the putative catalyst into the real one, due to significant chemical changes of the surface Pd species.

To elucidate the structure–activity relationship of the above alcohol oxidation, the isolated PdHAPs were characterized by XAFS and transmission electron microscopy (TEM). As shown in Figure 1, the Pd K-edge XANES spectrum of recovered PdHAP-0 (C) was similar to that of Pd foil (F). The FT of *k*³-weighted EXAFS exhibited a single peak at approximately 2.5 Å due to the contiguous Pd–Pd bond in the metallic form with a *R* and a CN of 2.76 Å and 10, respectively, as listed in Table 1 (sample C).¹⁸ The *R* value is consistent with that of Pd foil

(19) Tanaka, H.; Yasukawa, A.; Kandori, K.; Ishikawa, T. *Colloids Surf. A* **1997**, *125*, 53.

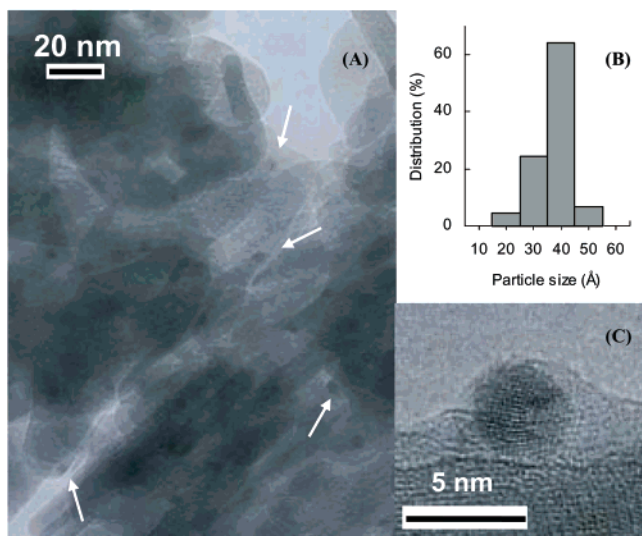


Figure 5. (A) TEM image, (B) size distribution diagram of the Pd nanoparticles, and (C) HR-TEM image of an eight-shell Pd nanocluster for the recovered PdHAP-0 catalyst after oxidation of 1-phenylethanol. Reaction was conducted with 1-phenylethanol (1 mmol), PdHAP-0 (0.1 g, Pd 2 μ mol) and trifluorotoluene (5 mL) at 90 °C for 1 h under an O₂ atmosphere.

(2.75 Å), whereas the CN value was smaller than that of Pd foil (12), which is due to the smaller particle size of the Pd nanoclusters. These results are in good agreement with those of the TEM analysis, where the Pd nanoclusters with a mean diameter (d) of ca. 38 Å having a narrow size distribution (standard deviation $\sigma = 5.7$ Å) were formed on PdHAP-0 (Figure 5A,B).²⁰ Because of the low level of Pd loading, the peaks attributable to the face-centered cubic (fcc) lattice could not be confirmed by XRD analysis. From high-resolution TEM analysis, however, the regular arrangement of Pd atoms on the Pd nanocluster surface can be clearly observed with 17 Pd atoms along the {111} planes (Figure 5C). Hence, the present nanoclusters have an fcc cuboctahedral shape with an eight-shell structure composed of ca. 2060 Pd atoms as the magic number.²¹ On the other hand, monomeric Pd^{II} species on PdHAP-1 are exceptionally stable against reducing reagents such as alcohols and molecular hydrogen.²² The XANES spectrum of recovered PdHAP-1 are identical to those of fresh PdHAP-0 and Pd oxide, revealing that electronic configuration of the Pd species did not change (Figure 1, compare spectra D and E). The curve-fitting analysis of the inverse FT could be completed by using two Pd–O bonds with the same distance and coordination numbers as those of the fresh one (Figure 2D and Table 1D).¹⁸ TEM examination also proved that there was no formation of Pd particles after the alcohol oxidation. From the above results, it can be concluded that the catalytically active

Table 3. Oxidation of Benzylic and Allylic Alcohols Catalyzed by PdHAP-0 with Molecular Oxygen^a

| entry | substrate | product | time (h) | conv. (%) ^b | yield (%) ^b |
|-------------------|-----------|---------|----------|------------------------|------------------------|
| 1 | | | 1 | >99 | 99 |
| 2 | | | 3 | >99 | 99 |
| 3 | | | 3 | >99 | 99 |
| 4 | | | 3 | 97 | 94 |
| 5 | | | 1 | >99 | 98 |
| 6 ^c | | | 2 | 98 | 97 |
| 7 | | | 10 | >99 | 99 |
| 8 | | | 24 | 92 | 91 |
| 9 | | | 24 | 90 | 87 |
| 10 ^{d,e} | | | 24 | >99 | 94 |
| 11 ^d | | | 6 | 91 | 87 |
| 12 ^d | | | 24 | 87 | 80 |
| 13 | | | 24 | 84 | 80 |

^a Reaction conditions: PdHAP-0 (0.1 g, Pd 0.2 mol %), alcohol (1 mmol), trifluorotoluene (5 mL), 90 °C, O₂ atmosphere. ^b Determined by GC analysis via an internal standard technique. ^c Under 1 atm of air instead of pure O₂. ^d Toluene (5 mL) was used as solvent. ^e PdHAP-0 (0.3 g, Pd 0.6 mol %).

species is not the original monomeric Pd^{II} species but the in situ generated Pd nanoparticles on the hydroxyapatite surface during the course of the alcohol oxidation.

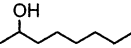
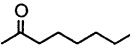
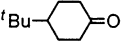
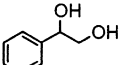
Aerobic Oxidation of Alcohols by the PdHAP-0 Catalyst.

The scope of the PdHAP-0 for a wide variety of alcohols was examined. The present catalyst system showed a higher reactivity for benzylic and allylic alcohols than for aliphatic ones. As can be seen from Table 3, various benzylic and allylic alcohols were selectively converted into the corresponding carbonyl compounds in excellent yields under 1 atm of O₂ pressure. Even under air conditions instead of pure O₂, the above oxidations proceeded smoothly; a quantitative yield of acetophenone was obtained within 2 h (entry 6). It is possible to synthesize dicarbonyl compounds, which are important building blocks for the synthesis of heterocyclic compounds, by the oxidation of α -hydroxyketones (entries 8 and 9).²³ In the case of cyclopropylphenyl carbinol, the oxidation of the hydroxyl group occurred without cleavage of the cyclopropyl ring (entry 10). In the

(23) Vollhardt, K. P. C.; Schore, N. E. *Organic Chemistry*, 2nd ed.; Freeman: New York, 1994; pp 924–929.

- (20) The Pd nanoclusters on the HAP surface have the narrowest size distribution with a standard deviation of 5.7 Å ($\sigma/d = 15\%$) among Pd/carbon ($d = 29$ Å), Pd/Al₂O₃ ($d = 32$ Å), and Pd/SiO₂ ($d = 47$ Å) catalysts whose σ/d values were between 26% and 30%. See Figure S4 in Supporting Information.
- (21) (a) Schmid, G. *Aspects of Homogeneous Catalysis*; Ugo, R., Ed.; Kluwer Academic Publishers: Dordrecht, The Netherlands, 1990; Vol. 7, p 1. (b) Benfield, R. E. *J. Chem. Soc., Faraday Trans.* **1992**, *88*, 1107. (c) Veisz, B.; Király, Z.; Tóth, L.; Pécz, B. *Chem. Mater.* **2002**, *14*, 2882.
- (22) We have recently reported that the chemisorbed PdCl₂ species on the PdHAP-0 was efficiently reduced to Pd nanoclusters with a mean diameter of 30 Å under H₂ atmosphere, which acted as an efficient heterogeneous catalyst for the deprotection of *N*-benzyloxycarbonyl group from amino acids. On the contrary, the above reaction hardly occurred in the presence of the PdHAP-1 without structural change around the Pd^{II} center. See Ref 16e.

Table 4. Oxidation of Various Alcohols Catalyzed by PdHAP-0 with Molecular Oxygen^a

| entry | substrate | product | time (h) | conv. (%) ^b | yield (%) ^b |
|-------------------|---|---|----------|------------------------|------------------------|
| 1 |  |  | 24 | 93 | 91 |
| 2 |  |  | 24 | 93 | 84 |
| 3 |  |  | 24 | 91 | 84 |
| 4 |  |  | 24 | 95 | 91 |
| 5 |  |  | 24 | 93 | 91 |
| 6 ^c |  |  | 12 | 97 | 94 |
| 7 ^c |  |  | 12 | 92 | 90 |
| 8 |  |  | 24 | >99 | 99 |
| 9 |  |  | 24 | 99 | 98 |
| 10 ^{c,d} |  |  | 24 | >99 | 96 |

^a Reaction conditions: PdHAP-0 (0.3 g, Pd 0.6 mol %), alcohol (1 mmol), trifluorotoluene (5 mL), 90 °C, O₂ atmosphere. ^b Determined by GC analysis via an internal standard technique. ^c PdHAP-0 (0.1 g, Pd 0.2 mol %). ^d 110 °C.

oxidation of α,β -unsaturated alcohols, C=C double bonds remained intact without an intramolecular hydrogen transfer (entries 11–13). Secondary linear and cyclic aliphatic alcohols were smoothly oxidized into the corresponding ketones, as summarized in Table 4. Especially, borneol and 2-adamantanol were successfully converted despite steric hindrance (entries 6 and 7). The PdHAP-0 catalyst was also applicable to the oxidation of heterocyclic alcohols, such as 2-thiophenemethanol and furfuryl alcohol, to afford the corresponding aldehydes in high yields (entries 8 and 9). In general, the previously reported monomeric transition metal complexes are unable to catalyze the oxidation of these alcohols containing heteroatoms, because the strong coordination to a metal center deactivates the catalysts. In the case of *vic*-diol of styrene glycol, carbon–carbon bond cleavage mainly took place to afford benzaldehyde as the major product and a trace amount of the corresponding diketone (entry 10). Unfortunately, cyclohexanol and 1-octanol proved to be poor substrates, yielding the corresponding carbonyl compounds in 34% and 10% yields for 24 h, respectively, even when 0.6 mol % Pd catalyst was employed.

The lifetime and leaching of active metal species into solution are important points to consider when heterogeneous catalysts are used, particularly for industrial and pharmaceutical application of alcohol oxidations.²⁴ To ensure that no deactivation occurred in the catalytic cycle, another portion of the alcohol was successively added to the reaction mixture after the first run. As shown in Figure 6, the second and third cycles for the oxidation of 1-phenylethanol proceeded efficiently without an

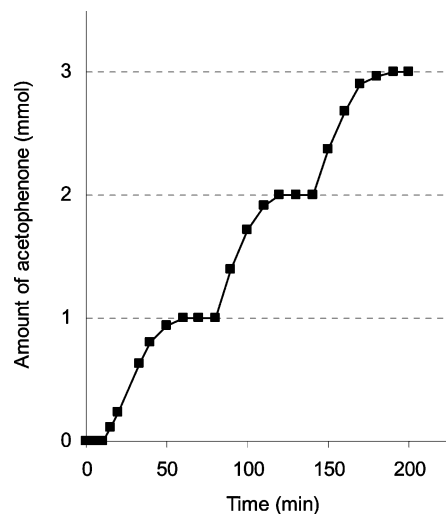


Figure 6. Time profile for the successive oxidation of 1-phenylethanol catalyzed by PdHAP-0. Reaction conditions: PdHAP-0 (0.1 g, Pd 2 μ mol), 1-phenylethanol (1 mmol), trifluorotoluene (5 mL), 90 °C, O₂ atmosphere.

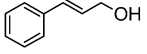
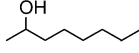
induction period, giving acetophenone in over 98% yields, respectively. Moreover, the catalyst was filtered off after ca. 50% conversion at the reaction temperature. Further treatment of the filtrate under similar reaction conditions did not afford any products. ICP analysis of the filtrate confirmed that the Pd content was below the detection limit. It can be said that the present alcohol oxidation undoubtedly proceeds on the Pd nanoclusters located on the hydroxyapatite surface. The reaction mixture was centrifuged after the first run for the recycling experiment, and the “spent” PdHAP-0 was removed from the solvent. When additional 1-phenylethanol and trifluorotoluene were added, both the second and third reactions gave acetophenone in over 97% yield.

With respect to the solvent effect on the oxidation of benzyl alcohol under the identical reaction conditions as used for entry 1 in Table 3, trifluorotoluene was the most effective solvent. Although a relatively high alcohol conversion of 65% was achieved in 1,2-dithoxyethane solvent, dibenzyl ether and benzyl benzoate were detected as side products in 16% and 10% yields, respectively. Also, aprotic polar solvents such as acetonitrile, dimethylformamide (DMF), and dimethyl sulfoxide (DMSO) were employed as reaction media, but they turned out to be not effective at all. This lack of activity might be explained by the coordination of heteroatoms to the Pd^{II} centers, thus preventing their reduction to Pd⁰. Due to increasing environmental consciousness, the use of water instead of organic solvents as a reaction medium is desirable, because water is a safe, economical, and environmentally benign solvent.²⁵ In addition, unique reactivity and selectivity that are not attained under dry conditions are often observed in aqueous reactions due to water’s hydrophobic and hydrogen-bonding effects.^{25b} It is noteworthy that the oxidation could be performed even under biphasic water–alcohol conditions owing to the high hydrophilic character of the hydroxyapatite.²⁶ For example, 1-phenylethanol in water with 0.04 mol % PdHAP-0 catalyst afforded acetophenone in a 94% yield for 24 h; the corresponding turnover number (TON) and turnover frequency (TOF) were

(25) For example, see (a) Li, C.-J., Chan, T.-H., Eds. *Organic Reactions in Aqueous Media*; Wiley: New York, 1997. (b) Kobayashi, S.; Manabe, K. *Acc. Chem. Res.* **2002**, *35*, 209. (c) Manabe, K.; Kobayashi, S. *Chem. Eur. J.* **2002**, *8*, 4095.

(24) Arends, I. W. C. E.; Sheldon, R. A. *Appl. Catal. A: Gen.* **2001**, *212*, 175.

Table 5. Aerobic Oxidation of Various Alcohols Catalyzed by PdHAP-0 in Water^a

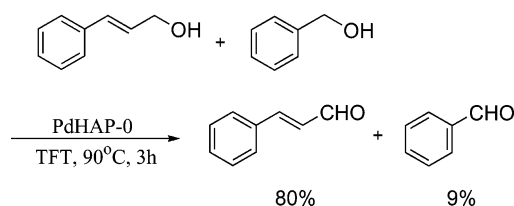
| entry | substrate | Pd (mol%) | conv. (%) ^b | yield (%) ^b |
|----------------|---|-----------|------------------------|------------------------|
| 1 ^c |  | 0.04 | >99 | 90 ^d |
| 2 |  | 0.04 | >99 | 94 |
| 3 ^c |  | 0.1 | 90 | 88 |
| 4 |  | 1 | 93 | 90 |
| 5 |  | 0.5 | 95 | 92 |

^a Reaction conditions: PdHAP-0 (0.1 g), alcohol (0.2–5 mmol), water (5 mL), 110 °C, O₂ atmosphere, 24 h. ^b Determined by GC analysis via an internal standard technique. ^c Aqueous NaOAc solution (0.2 M, 5 mL) was used as solvent. ^d Benzoic acid (10%) was formed.

2350 and 98 h⁻¹, respectively (Table 5, entry 2). Contrastingly, previously reported Pd catalyst systems of Pd(OAc)₂/PhenS*/NaOAc^{4i,1} and PS-PEG-supported Pd¹⁴ gave TONs of 170 and 20 and TOFs of 17 and 1 h⁻¹, respectively, for this substrate in water. It is also shown that conventional heterogeneous metal catalysts, such as Pd/carbon and Pt/carbon, promoted the oxidation of alcohols in an aqueous medium. However, the above carbon-supported metal catalysts oxidize only water-soluble carbohydrates as a substrate in the presence of one equivalent base.¹⁰

The applicability of the present synthetic protocol was highlighted by a 250-mmol scale oxidation of 1-phenylethanol employing 4 × 10⁻⁴ mol % Pd under solvent-free conditions. The oxidation was completed within 24 h, in which the TON of acetophenone based on Pd approached up to 236 000 with an excellent TOF of approximately 9800 h⁻¹. It is noteworthy that these TON and TOF values achieved by PdHAP-0 are significantly higher than those reported for other active catalyst systems, such as K₂[OsO₂(OH)₄] (TON and TOF respectively 16 600 and 700 h⁻¹),²⁷ Ru/Al₂O₃ (950 and 300 h⁻¹),^{9i,k} RuCl₂-(PPh₃)₃/TEMPO (466 and 104 h⁻¹),^{5k} Ru/quinone/Co-salene (194 and 97 h⁻¹),^{5l} Pd(IrPr)(OAc)₂(H₂O)/HOAc/MS3Å (1000 and 50 h⁻¹),^{4o} and Pd(OAc)₂/PhenS*/NaOAc (400 and 10 h⁻¹).⁴ⁱ Moreover, most reported catalyst systems require additional bases, electron/proton transfer mediators, and high O₂ pressure. Our PdHAP-0 catalyst does not need any additives or cocatalysts to facilitate its efficient catalytic cycle under an atmospheric O₂ pressure. *The present Pd catalytic system therefore provides an opportunity for simple and practical organic synthesis, meeting the increasing demands for environmentally friendly chemical processes.*

When an equimolar mixture of benzyl alcohol and 1-phenylethanol was used as substrate, the PdHAP-0 catalyst oxidized

Scheme 1

both alcohols at similar reaction rates to give the corresponding benzaldehyde and acetophenone in 93% and 95% yields, respectively. Furthermore, an intramolecular competitive oxidation of 4-(1-hydroxyethyl)benzyl alcohol proceeded at similar oxidizing rates for primary and secondary hydroxyls, giving 4-acetylbenzaldehyde in quantitative yield. The above results are in sharp contrast to those for monomeric Pd and Ru catalysts, in which the oxidation of primary benzylic alcohols proceeded faster than secondary ones.^{4l,5j,k,9k,16a} Alternatively, the PdHAP-0 catalyst prefers cinnamyl alcohol over benzyl alcohol in the intermolecular competitive reaction, affording an 80% yield of cinnamaldehyde together with only a 9% yield of benzaldehyde after 3 h, as shown in Scheme 1.²⁸ This catalytic behavior is analogous to those of the Pd nanoclusters such as Pd₅₆₁phen₆₀-(OAc)₁₈₀^{13a} and Pd₂₀₆₀(NO₃)₃₆₀(OAc)₃₆₀O₈₀^{13b} but is markedly distinct from those of the monomeric Ru and Pd catalysts. It is said that the monomeric Pd^{II} complex systems do not efficiently oxidize α,β-unsaturated alcohols because of the irreversible coordination of the C=C double bond to the Pd^{II} species.^{4h,n} Vide infra, this high reactivity toward cinnamyl alcohol is a result of the multiple interactions between the particle surface and allylic alcohols.

Size-Dependent Catalytic Activity of the Supported Pd Nanoclusters. Nanoscale transition metal clusters have attracted a great deal of attention as potentially advanced materials possessing unique electronic, optic, and magnetic properties as well as catalytic functions.²⁹ The general routes of nanocluster synthesis are based on the chemical reduction of transition metal salts with the appropriate reducing agents such as molecular hydrogen, hydrazine, and carbon monoxide in the presence of stabilizing ligands.³⁰ Achieving precise control of particle size and overall particle size distribution is one of the most important challenges to provide unique chemical and physical properties.^{14b} Vide supra, the Pd species of the fresh PdHAP-0 exist in a monomeric PdCl₂ structure grafted on hydroxyapatite surface. When the PdHAP-0 was employed as a catalyst for the aerobic oxidation of alcohol, such monomeric Pd^{II} species were easily reduced to Pd⁰ by alcohol substrates and then transformed into Pd nanoclusters. These findings prompted the further examination of the size-controlled synthesis of the Pd nanoclusters on the surface of hydroxyapatite by varying the kind of alcohol substrates.

Oxidations of 1-phenylethanol, benzyl alcohol, cinnamyl alcohol, and benzhydrol by use of 0.2 mol % PdHAP-0 were carried out at 90 °C, and then the recovered catalysts were

(26) Hydrophilic property of hydroxyapatite was evaluated by a simple adsorption technique. See Whitehurst, D. D. *CHEMTECH*, **1980**, *10*, 44. Hydroxyapatite (1.0 g) was dried at 573 K for 3 h, followed by exposure to air with high humidity. After 48 h, the hygroscopic degree (*H*) was calculated according to $H = [(X_w - X_d)/X_d] \times 100$ (*X_w*, weight of wet sample; *X_d*, weight of dried sample). The estimated hygroscopic degree of hydroxyapatite was 11.7.

(27) Döbler, C.; Mehlretter, G. M.; Sundermeier, U.; Eckert, M.; Militzer, H.-C.; Beller, M. *Tetrahedron Lett.* **2001**, *42*, 8447.

(28) Cinnamyl alcohol was more unfavorable to be oxidized than benzyl alcohol in separate experiments (entries 1 and 11 in Table 3).

(29) (a) Schmid, G. *Chem. Rev.* **1992**, *92*, 1709. (b) Schmid, G.; Chi, L. F. *Adv. Mater.* **1998**, *10*, 515. (c) Aiken, J. D.; Finke, R. G. *J. Mol. Catal. A: Chem.* **1999**, *145*, 1. (d) Rao, C. N. R.; Kulkarni, G. U.; Thomas, P. J.; Edwards, P. P. *Chem. Eur. J.* **2002**, *8*, 29.

(30) (a) *Clusters and Colloids: From Theory to Applications*; Schmid, G., Ed.; VCH: Weinheim, Germany, 1994. (b) *Nanoparticles and Nanostructured Films*; Fendler, J. H., Ed.; Wiley-VCH: Weinheim, Germany, 1998.

characterized by TEM. The mean diameters of Pd nanoclusters generated in each oxidation increased in the order benzyl alcohol (ca. 35 Å, $\sigma = 6.4$ Å) \approx 1-phenylethanol (ca. 38 Å, $\sigma = 5.7$ Å) as shown in Figure 5) < benzhydrol (ca. 78 Å, $\sigma = 20.2$ Å) \approx cinnamyl alcohol (ca. 79 Å, $\sigma = 18.0$ Å).¹⁸ The initial oxidation rates of the alcohols decreased as follows: benzyl alcohol ($6.54 \times 10^{-3} \text{ M}\cdot\text{min}^{-1}$) \approx 1-phenylethanol ($6.35 \times 10^{-3} \text{ M}\cdot\text{min}^{-1}$) > benzhydrol ($1.20 \times 10^{-3} \text{ M}\cdot\text{min}^{-1}$) \approx cinnamyl alcohol ($1.19 \times 10^{-3} \text{ M}\cdot\text{min}^{-1}$). Alcohol substrates with high reactivities tend to produce smaller diameters of Pd nanoclusters having narrow size distributions. Miyake and co-workers³¹ have succeeded in the size-controlled syntheses of Pd and Pt nanoclusters by varying the kind of alcohol substrates and/or their concentration in the presence of the protecting polymer, poly(*N*-vinyl-2-pyrrolidone) (PVP), where the diameters of nanoclusters decreased with increasing reduction rates of the metal ions. It can be said that kinetics of the reduction of metal ions by alcohol substrate plays a crucial role in determining the particle size. The rapid reduction generates more nuclei of Pd metals in a shorter period and efficiently suppresses the growth of metal nanoclusters.

Furthermore, the structure sensitivity of the Pd nanocluster catalysts for alcohol oxidation has been investigated by relating activity data to Pd⁰ nanocluster size.³² The particle surface is composed of different types of sites classified as high-coordination-number terrace atoms and low-coordination-number atoms (edge and corner). The relative proportion of these sites with respect to the total number of surface atoms is well-known to vary with the metal particle sizes. In an effort to examine the correlation between the amount of potentially active Pd sites and the catalytic activity for the alcohol oxidation, two representative Pd nanoclusters with mean diameters of 38 and 78 Å were prepared according to the above method, with 1-phenylethanol and benzhydrol as alcohol substrates, respectively. Assuming that the present Pd nanoparticles are cubooctahedral in shape with a cubic close-packed structure in this size range, the model of full-shell nanoparticles is adopted.^{21,33} The total number of the Pd atoms of nanocluster (N_T) can be calculated from

$$d_{\text{sph}} = 1.105d_{\text{at}}N_T^{1/3} \quad (2)$$

where d_{sph} is the mean diameter of the Pd crystallites obtained from TEM analysis and d_{at} is the atom diameter of Pd, 0.274 nm. The numbers of m and surface atoms (N_S) are also given by eqs 3 and 4, based on the values of N_T :

$$N_T = (10m^3 - 15m^2 + 11m - 3)/3 \quad (3)$$

$$N_S = 10m^2 - 20m + 12 \quad (4)$$

Moreover, the surface sites can be divided into the high-coordination-number site (N_{HS} , face atom only) and low-coordination-number sites (N_{LS} , edge and corner atom), according to

$$N_{\text{HS}} = 6(m - 2)^2 + 4(m - 3)(m - 2) \quad (5)$$

$$N_{\text{LS}} = 24(m - 2) + 12 \quad (6)$$

Table 6 summarizes the calculated geometric parameters for N_S , N_{HS} , and N_{LS} for 38 and 78 Å diameter Pd nanoclusters.

With two prepared Pd nanoclusters having different mean diameters, oxidations of 1-phenylethanol and benzhydrol were performed, and then initial oxidation rates were measured at ca. 10% conversion of alcohols. TEM analyses support that the size distributions remained virtually unchanged even after the above four experiments. To compare the catalytic activities, the TOF values were determined on the basis of the N_S , N_{HS} , and N_{LS} for each size of Pd nanoclusters, as listed in Table 7. If all surface atoms of the Pd nanoclusters act catalytically as the same active species for the alcohol oxidations, the TOF values normalized to N_S are expected to be independent of the Pd nanocluster sizes. As a result, the small nanocluster gives higher TOFs than the large nanocluster. In addition, the TOF values based on the terrace atoms (N_{HS}) depend on the cluster size. Upon consideration of the low-coordinated Pd atoms (N_{LS}) as catalytically active sites, the normalized TOF values were found to be independent of the Pd nanocluster sizes. It can be said that only the low-coordinated Pd atoms are responsible for the catalysis. Similar observations were reported in the Heck³⁴ and Suzuki³⁵ couplings with PVP-stabilized Pd nanoparticles and hydrogenation reaction by Pd-montmorillonite catalyst.^{21c} Therefore, this alcohol oxidation is considered "structure-sensitive" and the coordinately unsaturated Pd atoms act as the key active species within a regular arrangement of the Pd nanoclusters.

Mechanistic Investigations. The preliminary observations described below provide some insights into the oxidation pathway. Addition of a radical trap, 2,2',6,6'-tetramethylpiperidine *N*-oxyl (TEMPO), hardly influenced the oxidation rate of 1-phenylethanol. The oxidation of hydroxyls occurred exclusively without skeletal isomerization and carbon-carbon bond cleavage for radical clock substrates, such as cyclopropylphenyl carbinol and cyclobutanol (entry 10 in Table 3 and entry 2 in Table 4). Thus, the present catalytic system was determined not to contain free radical intermediates. In monitoring the O₂ uptake during the oxidation of 1-phenylethanol, the ratio of O₂ consumed to acetophenone was ca. 1:2, suggesting that molecular oxygen was quantitatively used for the oxidative dehydrogenation as an oxidant. Upon consideration of the above results as well as the insights obtained from the calculations on palladium crystallites, a possible reaction pathway on the surface of Pd⁰ nanoclusters is illustrated in Scheme 2. First, an oxidative addition of an O-H bond from alcohol to the coordinately unsaturated Pd⁰ species at the edge affords a Pd-alcoholate species, which undergoes a β -hydride elimination to produce the corresponding carbonyl compounds and a Pd-hydride species. The reaction of the hydride species with O₂ regenerates the Pd⁰ species, along with the formation of O₂ and H₂O. The reaction mixture at ca. 50% conversion was subjected to the qualitative test for H₂O₂ production. The color of KI-containing starch changed slightly from light yellow to blue, thus suggesting that H₂O₂ is a more likely intermediate for the formation of O₂

(31) (a) Teranishi, T.; Miyake, M. *Chem. Mater.* **1998**, *10*, 594. (b) Teranishi, T.; Hosoe, M.; Tanaka, T.; Miyake, M. *J. Phys. Chem. B* **1999**, *103*, 3818.

(32) Van Hardeveld, R.; Hartog, F. *Surf. Sci.* **1969**, *15*, 189.

(33) It should be noted that although the particles have a size distribution, the mean diameters of particles were employed for the calculations of the geometric parameters such as N_T , N_S , N_{HS} , and N_{LS} . A similar approximation has been carried out in the studies of particle size effect on Heck and Suzuki coupling reactions. See refs 34b and 35.

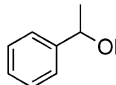
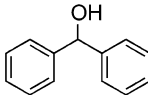
(34) (a) Augustine, R. L.; O'Leary, S. T. *J. Mol. Catal. A: Chem.* **1995**, *95*, 277. (b) Le Bars, J.; Specht, U.; Bradley, J. S.; Blackmond, D. G. *Langmuir* **1999**, *15*, 7621.

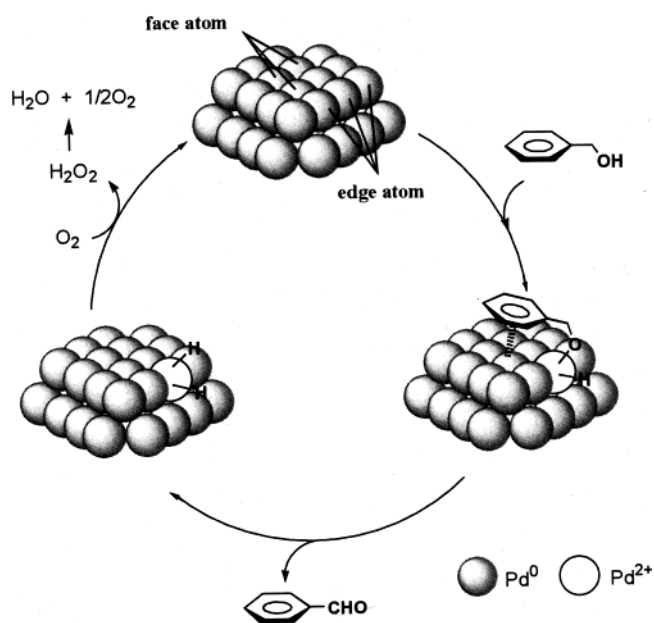
(35) Li, Y.; Boone, E.; El-Sayed, M. A. *Langmuir* **2002**, *18*, 4921.

Table 6. Correlation between the Size of Nanocluster and N_S , N_{HS} , and N_{LS} in the Reaction Mixture

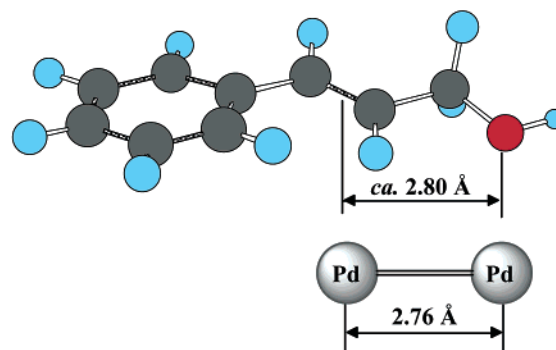
| geometric parameters ^a | diameter (Å) | |
|--|--------------|--------|
| | 38 | 78 |
| total number of atoms N_T | 2057 | 1788.5 |
| number of surface atoms N_S | 642 | 2892 |
| number of terrace sites N_{HS} | 462 | 2496 |
| number of low-coordination sites N_{LS} | 180 | 396 |
| number of edge sites N_E | 168 | 384 |
| number of corner sites N_C | 12 | 12 |
| moles of Pd atoms in the reaction mixture $\times 10^6$ | 2.00 | 2.00 |
| moles of Pd clusters in the reaction mixture $\times 10^{10}$ | 9.72 | 1.12 |
| number of N_S in the reaction mixture $\times 10^7 \times L^{-1}$ | 6.24 | 3.24 |
| number of N_{HS} in the reaction mixture $\times 10^7 \times L^{-1}$ | 4.49 | 2.80 |
| number of N_{LS} in the reaction mixture $\times 10^7 \times L^{-1}$ | 1.75 | 0.44 |
| number of N_E in the reaction mixture $\times 10^7 \times L^{-1}$ | 1.63 | 0.43 |
| number of N_C in the reaction mixture $\times 10^7 \times L^{-1}$ | 0.12 | 0.01 |

^a L = Avogadro's constant.**Table 7.** Initial TOF Values Based on N_S , N_{HS} , and N_{LS} ^a

| substrate | diameter of Pd nanocluster (Å) | TOF (h^{-1}) $\times 10^{-3}$ | | |
|---|--------------------------------|-----------------------------------|----------|----------|
| | | N_S | N_{HS} | N_{LS} |
|  | 38 | 1.01 | 1.41 | 3.61 |
| | 78 | 0.34 | 0.39 | 2.50 |
|  | 38 | 0.12 | 0.16 | 0.41 |
| | 78 | 0.05 | 0.06 | 0.36 |

^a N_S , number of surface atoms, N_{HS} , number of terrace sites, N_{LS} , number of low-coordination sites.**Scheme 2.** Possible Reaction Mechanism for the Oxidation of Alcohols on the Surface of Pd Nanocluster

and H_2O (Scheme 2).^{4k} The kinetic isotope effect for the intramolecular competitive oxidation of α -deuterio-*p*-methylbenzyl alcohol gave a k_H/k_D value of 2.0 at 90 °C, which is consistent with those obtained for other systems ($k_H/k_D = 1.3$ – 2.5).^{4l,m,7c,g,36} This implies that the elimination of β -hydride from the Pd-alcoholate species may be a rate-determining step.

**Figure 7.** Schematic representation of the multiple interaction between Pd–Pd paired site and cinnamyl alcohol.

Furthermore, the initial oxidation rates of 1-phenylethanol were independent of the O_2 pressure; the normalized initial oxidation rate at 0.2 (air), 2, and 3 atm of molecular oxygen based on that at 1 atm were 0.98, 1.04, and 1.03, respectively.¹⁸ In relation to this, the byproducts of hydrogenation and isomerization, which are induced by the Pd-hydride species, could hardly be detected in the oxidation of α,β -unsaturated alcohols (entries 11–13 in Table 3). This is clear evidence for the high reactivity of the Pd-hydride species toward molecular oxygen.

With respect to the above oxidation mechanism, we point out the participation of multiple interactions between a Pd–Pd paired site and an alcohol substrate.¹³ *Vide supra*, the high reactivity toward the cinnamyl alcohol over benzyl alcohol in the intermolecular competitive oxidation could be ascribed to the high coordination ability of a C=C double bond of the cinnamyl alcohol to the Pd species as an anchor, which could also enhance the interaction of the hydroxyl group with a neighboring Pd species resulting in the exclusive formation of cinnamaldehyde. Indeed, the distance of the Pd–Pd bond (2.76 Å) determined by EXAFS analysis is in accordance with the distance between the center of a C=C bond and an oxygen atom for the O–H group of cinnamyl alcohol (ca. 2.8 Å), as depicted in Figure 7.³⁷ The multiple interaction also accounts for the higher reactivity of benzylic alcohols when compared with aliphatic ones,³⁸ where the electron donation effect of the adsorbed aryl ring to the Pd nanocluster surface through the π -bond interaction facilitates the rupture of the O–H bond by a neighboring coordinately unsaturated Pd species to form a Pd-alcoholate species.³⁹ These cooperative actions could not be attained with single-site Pd catalysts, which can explain the prominent activity of the Pd nanocluster catalysts for the oxidation of alcohols.

Conclusions

On the basis of characterization by physicochemical methods, it was found that monomeric $PdCl_2$ species could be grafted on the surface of stoichiometric hydroxyapatite. When PdHAP-0 was used as a catalyst for aerobic alcohol oxidation, an induction period was observed and Pd nanoclusters were generated under

- (36) (a) Ozawa, F.; Ito, T.; Yamamoto, A. *J. Am. Chem. Soc.* **1980**, *102*, 6457. (b) Noronha, G.; Henry, P. M. *J. Mol. Catal. A* **1997**, *140*, 75.
 (37) The distance between the center of a C=C bond and an oxygen atom of the O–H group of cinnamyl alcohol was calculated by the PM3 semiempirical method as implemented in MOPAC.
 (38) The single-site Pd catalysts oxidized both benzylic and aliphatic alcohols at almost similar reaction rates. See ref 4h,n.
 (39) This is analogous to the acceleration of oxidative addition of aryl halides to Pd^0 species by use of aryl halides with electron-withdrawing substituents and/or electron-donating phosphate ligands.

the reaction conditions without stabilizing ligands, as confirmed by TEM and Pd K-edge XAFS analyses. Such in situ generated Pd nanoclusters can offer an extremely simple and highly efficient heterogeneous catalyst system for the oxidation of alcohols by molecular oxygen. It is free of additives and cocatalysts, recyclable, and tolerates several substrates, which makes it an ideal environmentally benign chemical process in terms of potential industrial application for this transformation. Further demonstrated was a convenient approach to control the size of Pd nanoparticles on hydroxyapatite surfaces by varying the kind of alcohol substrates in the oxidation reactions. The good correlation between the normalized TOF values and the low-coordination sites suggests that the oxidation of alcohols may occur primarily at the coordinately unsaturated Pd atoms on the surface of the nanoclusters.

Experimental Section

Materials. PdCl₂ was obtained from N. E. Chemcat Co. Ltd. and used without further purification. (NH₄)₂HPO₄ and Ca(NO₃)₂·4H₂O were purchased from Wako Pure Chemical Ind., Ltd. Solvents and all commercially available alcohols were purified by standard procedures used before. α -Deuterio-*p*-methylbenzyl alcohol and 4-(1-hydroxyethyl)-benzyl alcohol were synthesized by the reduction of *p*-methylbenzaldehyde and 4-acetylbenzoic acid according to literature procedures.^{5k}

Synthesis of Hydroxyapatite-Supported Pd Catalysts. (NH₄)₂-HPO₄ (40.0 mmol) was dissolved in deionized water (150 mL) and the pH was adjusted to 11 with aqueous NH₃ solution. To a solution of Ca(NO₃)₂·4H₂O (66.7 mmol) in deionized water (120 mL) adjusted to pH 11 with aqueous NH₃ solution was added dropwise over 30 min the above solution with vigorous stirring at room temperature, and then the obtained milky solution was heated at 90 °C for 10 min. The precipitate was filtered, washed with deionized water, and dried at 110 °C, giving stoichiometric hydroxyapatite, Ca₁₀(PO₄)₆(OH)₂ (HAP-0). Ca-deficient hydroxyapatite, Ca₉(HPO₄)(PO₄)₅(OH) (HAP-1), was also prepared by changing the Ca/P ratio from 1.67 to 1.50 in the above starting solutions. HAP-0 (2.0 g) was stirred at 25 °C for 3 h in 150 mL of acetone solution of PdCl₂(PhCN)₂ (2.67 × 10⁻⁴ M). The obtained slurry was filtered, washed with acetone, and dried under vacuum, yielding 2.01 g of PdHAP-0 (Pd content 0.02 mmol·g⁻¹). PdHAP-1 was also prepared by the same method with HAP-1 in place of HAP-0.

Typical Example for Oxidation of Alcohols. Into a reaction vessel with a reflux condenser were placed PdHAP-0 (0.1 g, Pd 2 μ mol), 1-phenylethanol (0.12 g, 1 mmol), and trifluorotoluene (5 mL). The resulting mixture was stirred at 90 °C under 1 atm of O₂. The progress of reaction was monitored by GC analysis. After 1 h, 98% yield of acetophenone was obtained. The amount of O₂ uptake was volumetrically measured by a gas buret directly connected to the rotary vacuum pump.

Typical Example for Oxidation of Alcohols in Water. Into a reaction vessel with a reflux condenser were placed PdHAP-0 (0.1 g, Pd 2 μ mol), 1-phenylethanol (0.6 g, 5 mmol), and water (5 mL). The resulting mixture was stirred at 110 °C under 1 atm of O₂. The progress of reaction was monitored by GC analysis. After 24 h, 94% yield of acetophenone was obtained.

Procedure for Large-Scale Oxidation of 1-Phenylethanol. Into a reaction vessel with a reflux condenser were placed 1-phenylethanol (30.5 g, 250 mmol) and PdHAP-0 (0.05 g, Pd 1 μ mol). The resulting mixture was stirred at 160 °C in the presence of O₂ under Dean–Stark conditions. After 24 h, PdHAP-0 was separated by filtration, and then distillation of the filtrate gave pure acetophenone (28.3 g, 94% yield).

Characterization. Powder X-ray diffraction patterns were recorded on a Philips X'Pert-MPD with Cu K α radiation. X-ray photoelectron spectroscopy was measured on a Shimadzu ESCA-KM with MgK α radiation. Energy-dispersive X-ray measurement was performed by Philips EDAX DX-4 attached to SEM. Infrared spectra were obtained with a Jasco FTIR-410. Elemental analysis was carried out on a Perkin-Elmer 2400CHN. Inductively coupled plasma measurement was performed by Nippon Jarrell-Ash ICAP-575 Mark II. X-ray absorption spectra were recorded by a fluorescence-yield collection technique at the beam line 01B1 station with attached Si(311) monochromator at SPring-8, JASRI, Harima, Japan (prop. 2001A0563-UX-np). Fluorescence yield was collected at room temperature by use of the 19-element solid-state detector. Data reductions were performed with the FACOM M-780 computer system of the Data Processing Center of Kyoto University. The detailed procedure for data analysis was described elsewhere.⁴⁰ HR-TEM micrographs were obtained with Hitachi Hf-2000 FE-TEM equipped with Kevex energy-dispersive X-ray detector operated at 200 kV.

Acknowledgment. We thank Dr. Takashi Yamamoto (Tokyo Institute Technology) and Dr. Tomoya Uruga (JASRI) for XAFS measurement and Dr. Tomoki Akita (Osaka National Research Institute AIST) for TEM measurement. K.M. thanks the JSPS Research Fellowships for Young Scientists. T.H. expresses his special thanks for the center of excellence (21COE) program Creation of Integrated Ecochemistry of Osaka University.

Supporting Information Available: Curve fitting analysis, TEM images, and effect of O₂ pressure on reaction rates. This material is available free of charge via the Internet at <http://pubs.acs.org>.

JA0488683

(40) Tanaka, T.; Yamashita, H.; Tsuchitani, R.; Funabiki, T.; Yoshida, S. *J. Chem. Soc., Faraday Trans.* **1988**, *84*, 2987.